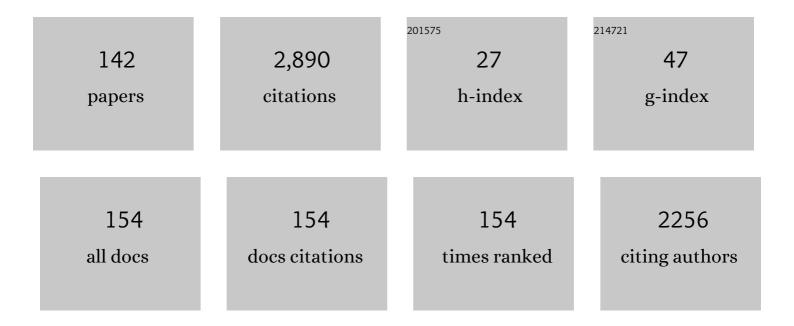
Atsushi Kumamoto

List of Publications by Year in descending order

Source: https://exaly.com/author-pdf/4305209/publications.pdf Version: 2024-02-01



#	Article	IF	CITATIONS
1	The Space Physics Environment Data Analysis System (SPEDAS). Space Science Reviews, 2019, 215, 9.	3.7	332
2	Lunar Radar Sounder Observations of Subsurface Layers Under the Nearside Maria of the Moon. Science, 2009, 323, 909-912.	6.0	166
3	Pulsating aurora from electron scattering by chorus waves. Nature, 2018, 554, 337-340.	13.7	149
4	The Plasma Wave Experiment (PWE) on board the Arase (ERG) satellite. Earth, Planets and Space, 2018, 70, .	0.9	124
5	Highâ€speed solar wind with southward interplanetary magnetic field causes relativistic electron flux enhancement of the outer radiation belt via enhanced condition of whistler waves. Geophysical Research Letters, 2013, 40, 4520-4525.	1.5	117
6	High Frequency Analyzer (HFA) of Plasma Wave Experiment (PWE) onboard the Arase spacecraft. Earth, Planets and Space, 2018, 70, .	0.9	93
7	Onboard software of Plasma Wave Experiment aboard Arase: instrument management and signal processing of Waveform Capture/Onboard Frequency Analyzer. Earth, Planets and Space, 2018, 70, .	0.9	64
8	Detection of Intact Lava Tubes at Marius Hills on the Moon by SELENE (Kaguya) Lunar Radar Sounder. Geophysical Research Letters, 2017, 44, 10,155.	1.5	62
9	Direct observations of asteroid interior and regolith structure: Science measurement requirements. Advances in Space Research, 2018, 62, 2141-2162.	1.2	54
10	Instrumentation and observation target of the Lunar Radar Sounder (LRS) experiment on-board the SELENE spacecraft. Earth, Planets and Space, 2008, 60, 321-332.	0.9	53
11	The Lunar Radar Sounder (LRS) Onboard theÂKAGUYA (SELENE) Spacecraft. Space Science Reviews, 2010, 154, 145-192.	3.7	50
12	Wire Probe Antenna (WPT) and Electric Field Detector (EFD) of Plasma Wave Experiment (PWE) aboard the Arase satellite: specifications and initial evaluation results. Earth, Planets and Space, 2017, 69, .	0.9	49
13	The Plasma Wave Investigation (PWI) onboard the BepiColombo/MMO: First measurement of electric fields, electromagnetic waves, and radio waves around Mercury. Planetary and Space Science, 2010, 58, 238-278.	0.9	44
14	Asymmetry of occurrence-frequency and intensity of AKR between summer polar region and winter polar region sources. Geophysical Research Letters, 1998, 25, 2369-2372.	1.5	42
15	Magnetic conjugate observation of theF3layer using the SEALION ionosonde network. Geophysical Research Letters, 2007, 34, .	1.5	42
16	Akebono observations of EMIC waves in the slot region of the radiation belts. Geophysical Research Letters, 2013, 40, 5587-5591.	1.5	40
17	Penetration of MeV electrons into the mesosphere accompanying pulsating aurorae. Scientific Reports, 2021, 11, 13724.	1.6	37
18	Visualization of rapid electron precipitation via chorus element wave–particle interactions. Nature Communications, 2019, 10, 257.	5.8	35

#	Article	IF	CITATIONS
19	The Characteristics of EMIC Waves in the Magnetosphere Based on the Van Allen Probes and Arase Observations. Journal of Geophysical Research: Space Physics, 2021, 126, e2020JA029001.	0.8	35
20	Effect of the solar wind proton entry into the deepest lunar wake. Geophysical Research Letters, 2010, 37, .	1.5	34
21	SC related electric and magnetic field phenomena observed by the Akebono satellite inside the plasmasphere. Earth, Planets and Space, 2004, 56, 269-282.	0.9	33
22	The Energization and Radiation in Geospace (ERG) Project. Geophysical Monograph Series, 0, , 103-116.	0.1	33
23	Multiple time-scale beats in aurora: precise orchestration via magnetospheric chorus waves. Scientific Reports, 2020, 10, 3380.	1.6	33
24	Solar zenith angle dependence of plasma density and temperature in the polar cap ionosphere and low-altitude magnetosphere during geomagnetically quiet periods at solar maximum. Journal of Geophysical Research, 2011, 116, n/a-n/a.	3.3	32
25	Distribution of the subsurface reflectors of the western nearside maria observed from Kaguya with Lunar Radar Sounder. Geophysical Research Letters, 2009, 36, .	1.5	31
26	Magnetic Search Coil (MSC) of Plasma Wave Experiment (PWE) aboard the Arase (ERG) satellite. Earth, Planets and Space, 2018, 70, .	0.9	31
27	SAPS measurements around the magnetic equator by CRRES. Geophysical Research Letters, 2008, 35, .	1.5	30
28	Detectability of subsurface interfaces in lunar maria by the LRS/SELENE sounding radar: Influence of mineralogical composition. Geophysical Research Letters, 2010, 37, .	1.5	29
29	Electrostatic Electron Cyclotron Harmonic Waves as a Candidate to Cause Pulsating Auroras. Geophysical Research Letters, 2018, 45, 12,661.	1.5	29
30	Estimation of the permittivity and porosity of the lunar uppermost basalt layer based on observations of impact craters by SELENE. Journal of Geophysical Research E: Planets, 2013, 118, 1453-1467.	1.5	27
31	Response of the Ionosphereâ€Plasmasphere Coupling to the September 2017 Storm: What Erodes the Plasmasphere so Severely?. Space Weather, 2019, 17, 861-876.	1.3	25
32	Seasonal and solar cycle variations of the vertical distribution of the occurrence probability of auroral kilometric radiation sources and of upflowing ion events. Journal of Geophysical Research, 2003, 108, .	3.3	24
33	Storm-time electric field distribution in the inner magnetosphere. Geophysical Research Letters, 2006, 33, .	1.5	24
34	Microscopic Observations of Pulsating Aurora Associated With Chorus Element Structures: Coordinated Arase Satelliteâ€₽WING Observations. Geophysical Research Letters, 2018, 45, 12,125.	1.5	24
35	Statistical analysis of the ionization ledge in the equatorial ionosphere observed from topside sounder satellites. Journal of Atmospheric and Solar-Terrestrial Physics, 2006, 68, 1340-1351.	0.6	23
36	Observations of veryâ€lowâ€energy (<10 eV) ion outflows dominated by O ⁺ ions in the region of enhanced electron density in the polar cap magnetosphere during geomagnetic storms. Journal of Geophysical Research, 2010, 115, .	3.3	23

#	Article	IF	CITATIONS
37	Observations and model calculations of theF3layer in the Southeast Asian equatorial ionosphere. Journal of Geophysical Research, 2011, 116, .	3.3	23
38	Synthetic Aperture Radar Processing of Kaguya Lunar Radar Sounder Data for Lunar Subsurface Imaging. IEEE Transactions on Geoscience and Remote Sensing, 2012, 50, 2161-2174.	2.7	23
39	Type-II entry of solar wind protons into the lunar wake: Effects of magnetic connection to the night-side surface. Planetary and Space Science, 2013, 87, 106-114.	0.9	23
40	Evolution of ring current and radiation belt particles under the influence of storm-time electric fields. Journal of Geophysical Research, 2007, 112, n/a-n/a.	3.3	22
41	Plasma wave observation using waveform capture in the Lunar Radar Sounder on board the SELENE spacecraft. Earth, Planets and Space, 2008, 60, 341-351.	0.9	22
42	lonization ledge structures observed in the equatorial anomaly region by using PPS system on-board the Ohzora (EXOS-C) satellite. Earth, Planets and Space, 2004, 56, e21-e24.	0.9	21
43	Comprehensive Observations of Substormâ€Enhanced Plasmaspheric Hiss Generation, Propagation, and Dissipation. Geophysical Research Letters, 2020, 47, e2019GL086040.	1.5	21
44	Seasonal variations of the electron density distribution in the polar region during geomagnetically quiet periods near solar maximum. Journal of Geophysical Research, 2009, 114, .	3.3	20
45	Plasma Wave Investigation (PWI) Aboard BepiColombo Mio on the Trip to the First Measurement of Electric Fields, Electromagnetic Waves, and Radio Waves Around Mercury. Space Science Reviews, 2020, 216, 1.	3.7	20
46	Electrodynamics in the duskside inner magnetosphere and plasmasphere during a super magnetic storm on March 13–15, 1989. Earth, Planets and Space, 2005, 57, 643-659.	0.9	19
47	Longitudinal Structure of Oxygen Torus in the Inner Magnetosphere: Simultaneous Observations by Arase and Van Allen Probe A. Geophysical Research Letters, 2018, 45, 10,177.	1.5	18
48	Conjugate Observations of Dayside and Nightside VLF Chorus and QP Emissions Between Arase (ERG) and Kannuslehto, Finland. Journal of Geophysical Research: Space Physics, 2020, 125, e2019JA026663.	0.8	18
49	Mare volcanism: Reinterpretation based on Kaguya Lunar Radar Sounder data. Journal of Geophysical Research E: Planets, 2014, 119, 1037-1045.	1.5	17
50	Deformation of Electron Pitch Angle Distributions Caused by Upper Band Chorus Observed by the Arase Satellite. Geophysical Research Letters, 2018, 45, 7996-8004.	1.5	17
51	Temporal and Spatial Variations of Storm Time Midlatitude Ionospheric Trough Based on Global GNSSâ€TEC and Arase Satellite Observations. Geophysical Research Letters, 2018, 45, 7362-7370.	1.5	17
52	Coincident Observations by the Kharkiv IS Radar and Ionosonde, DMSP and Arase (ERG) Satellites, and FLIP Model Simulations: Implications for the NRLMSISEâ€00 Hydrogen Density, Plasmasphere, and Ionosphere. Geophysical Research Letters, 2018, 45, 8062-8071.	1.5	17
53	Oxygen torus and its coincidence with EMIC wave in the deep inner magnetosphere: Van Allen Probe B and Arase observations. Earth, Planets and Space, 2020, 72, 111.	0.9	17
54	Sudden commencements related plasma waves observed by the Akebono satellite in the polar region and inside the plasmasphere region. Journal of Geophysical Research, 2003, 108, .	3.3	16

#	Article	IF	CITATIONS
55	Instantaneous Frequency Analysis on Nonlinear EMIC Emissions: Arase Observation. Geophysical Research Letters, 2018, 45, 13,199.	1.5	13
56	Temporal and Spatial Correspondence of Pc1/EMIC Waves and Relativistic Electron Precipitations Observed With Groundâ€Based Multiâ€Instruments on 27 March 2017. Geophysical Research Letters, 2018, 45, 13,182.	1.5	13
57	Evening Side EMIC Waves and Related Proton Precipitation Induced by a Substorm. Journal of Geophysical Research: Space Physics, 2021, 126, e2020JA029091.	0.8	13
58	Plasma Waves and Sounder (PWS) experiment onboard the Planet-B Mars orbiter. Earth, Planets and Space, 1998, 50, 213-221.	0.9	12
59	Simulation of mode conversion process from upper-hybrid waves to LO-mode waves in the vicinity of the plasmapause. Annales Geophysicae, 2010, 28, 1289-1297.	0.6	12
60	Horizontal structure of sporadic <i>E</i> layer observed with a rocketâ€borne magnesium ion imager. Journal of Geophysical Research, 2010, 115, .	3.3	12
61	Relationship Between the Locations of the Midlatitude Trough and Plasmapause Using GNSSâ€TEC and Arase Satellite Observation Data. Journal of Geophysical Research: Space Physics, 2021, 126, e2020JA028943.	0.8	12
62	Relation of the Plasmapause to the Midlatitude Ionospheric Trough, the Subâ€Auroral Temperature Enhancement and the Distribution of Smallâ€Scale Field Aligned Currents as Observed in the Magnetosphere by THEMIS, RBSP, and Arase, and in the Topside Ionosphere by Swarm. Journal of Geophysical Research: Space Physics, 2022, 127, .	0.8	12
63	Auroral kilometric radiation activity during magnetically quiet periods. Journal of Geophysical Research, 2005, 110, .	3.3	11
64	Auroral radio emission and absorption of medium frequency radio waves observed in Iceland. Earth, Planets and Space, 2008, 60, 207-217.	0.9	11
65	Cross-Energy Couplings from Magnetosonic Waves to Electromagnetic Ion Cyclotron Waves through Cold Ion Heating inside the Plasmasphere. Physical Review Letters, 2021, 127, 245101.	2.9	11
66	Temporal variations and spatial extent of the electron density enhancements in the polar magnetosphere during geomagnetic storms. Journal of Geophysical Research, 2010, 115, .	3.3	10
67	Density Depletions Associated With Enhancements of Electron Cyclotron Harmonic Emissions: An ERG Observation. Geophysical Research Letters, 2018, 45, 10,075.	1.5	10
68	Investigation of Small‣cale Electron Density Irregularities Observed by the Arase and Van Allen Probes Satellites Inside and Outside the Plasmasphere. Journal of Geophysical Research: Space Physics, 2021, 126, e2020JA027917.	0.8	10
69	Collaborative Research Activities of the Arase and Van Allen Probes. Space Science Reviews, 2022, 218, .	3.7	10
70	Largeâ€amplitude wave electric field in the inner magnetosphere during substorms. Journal of Geophysical Research, 2008, 113, .	3.3	9
71	Statistical study of polar distribution of mesoscale fieldâ€aligned currents. Journal of Geophysical Research, 2008, 113, .	3.3	9
72	Mission Data Processor Aboard the BepiColombo Mio Spacecraft: Design and Scientific Operation Concept. Space Science Reviews, 2020, 216, 1.	3.7	9

#	Article	IF	CITATIONS
73	Sheath capacitance observed by impedance probes onboard sounding rockets: Its application to ionospheric plasma diagnostics. Earth, Planets and Space, 2010, 62, 579-587.	0.9	8
74	Lunar ionosphere exploration method using auroral kilometric radiation. Earth, Planets and Space, 2011, 63, 47-56.	0.9	8
75	Strong Diffusion of Energetic Electrons by Equatorial Chorus Waves in the Midnightâ€toâ€Dawn Sector. Geophysical Research Letters, 2019, 46, 12685-12692.	1.5	8
76	Automatic Electron Density Determination by Using a Convolutional Neural Network. IEEE Access, 2019, 7, 163384-163394.	2.6	8
77	Plasma and Field Observations in the Magnetospheric Source Region of a Stable Auroral Red (SAR) Arc by the Arase Satellite on 28 March 2017. Journal of Geophysical Research: Space Physics, 2020, 125, e2020JA028068.	0.8	8
78	Spatial Extent of Quasiperiodic Emissions Simultaneously Observed by Arase and Van Allen Probes on 29 November 2018. Journal of Geophysical Research: Space Physics, 2020, 125, e2020JA028126.	0.8	8
79	Polarization observations of 4 <i>f_{ce}</i> auroral roar emissions. Geophysical Research Letters, 2015, 42, 249-255.	1.5	7
80	Observation of wakeâ€induced plasma waves around an ionospheric sounding rocket. Journal of Geophysical Research: Space Physics, 2015, 120, 5160-5175.	0.8	7
81	Direct Comparison Between Magnetospheric Plasma Waves and Polar Mesosphere Winter Echoes in Both Hemispheres. Journal of Geophysical Research: Space Physics, 2019, 124, 9626-9639.	0.8	7
82	The MEFISTO and WPT Electric Field Sensors of the Plasma Wave Investigation on the BepiColombo Mio Spacecraft. Space Science Reviews, 2020, 216, 1.	3.7	7
83	Multiâ€Event Analysis of Plasma and Field Variations in Source of Stable Auroral Red (SAR) Arcs in Inner Magnetosphere During Nonâ€Stormâ€Time Substorms. Journal of Geophysical Research: Space Physics, 2021, 126, e2020JA029081.	0.8	7
84	Multipoint Measurement of Fine‣tructured EMIC Waves by Arase, Van Allen Probe A and Ground Stations. Geophysical Research Letters, 2021, 48, e2021GL096488.	1.5	7
85	Electrostatic electron cyclotron harmonic waves observed by the Akebono satellite near the equatorial region of the plasmasphere. Earth, Planets and Space, 2007, 59, 613-629.	0.9	6
86	Stormâ€ŧime electron density enhancement in the cleft ion fountain. Journal of Geophysical Research, 2012, 117, .	3.3	6
87	The layered structure of lunar maria: Identification of the HF-radar reflector in Mare Serenitatis using multiband optical images. Icarus, 2012, 218, 506-512.	1.1	6
88	GENERATION MECHANISM OF THE SLOWLY DRIFTING NARROWBAND STRUCTURE IN THE TYPE IV SOLAR RADIO BURSTS OBSERVED BY AMATERAS. Astrophysical Journal, 2014, 787, 45.	1.6	6
89	Hectometric Line Spectra Detected by the Arase (ERG) Satellite. Geophysical Research Letters, 2018, 45, 11,555.	1.5	6
90	A Concise Empirical Formula for the Fieldâ€Aligned Distribution of Auroral Kilometeric Radiation Based on Arase Satellite and Van Allen Probes. Geophysical Research Letters, 2021, 48, e2021GL092805.	1.5	6

#	Article	IF	CITATIONS
91	Estimation of bulk permittivity of the Moon's surface using Lunar Radar Sounder on-board Selenological and Engineering Explorer. Earth, Planets and Space, 2020, 72, .	0.9	6
92	A Statistical Study of the Solar Wind Dependence of Multiâ€Harmonic Toroidal ULF Waves Observed by the Arase Satellite. Journal of Geophysical Research: Space Physics, 2022, 127, .	0.8	6
93	Electromagnetic compatibility (EMC) evaluation of the SELENE spacecraft for the lunar radar sounder (LRS) observations. Earth, Planets and Space, 2008, 60, 333-340.	0.9	5
94	Jovian slowâ \in drift shadow events. Journal of Geophysical Research, 2010, 115, .	3.3	5
95	Energetic Electron Precipitation Associated With Pulsating Aurora Observed by VLF Radio Propagation During the Recovery Phase of a Substorm on 27 March 2017. Geophysical Research Letters, 2018, 45, 12,651.	1.5	5
96	Impulsively Excited Nightside Ultralow Frequency Waves Simultaneously Observed on and off the Magnetic Equator. Geophysical Research Letters, 2018, 45, 7918-7926.	1.5	5
97	Effect of crack direction around laboratory-scale craters on material bulk permittivity. Icarus, 2019, 319, 512-524.	1.1	5
98	An Ephemeral Red Arc Appeared at 68° MLat at a Pseudo Breakup During Geomagnetically Quiet Conditions. Journal of Geophysical Research: Space Physics, 2020, 125, e2020JA028468.	0.8	5
99	Plasmasphere electron temperature structures. Advances in Space Research, 2004, 34, 2010-2015.	1.2	4
100	Enhancements of magnetospheric convection electric field associated with sudden commencements in the inner magnetosphere and plasmasphere regions. Advances in Space Research, 2006, 38, 1595-1607.	1.2	4
101	Impact of lithium releases on ionospheric electron density observed by impedance probe during WIND campaign. Earth, Planets and Space, 2010, 62, 589-597.	0.9	4
102	Narrowband frequency-drift structures in solar type IV bursts. Earth, Planets and Space, 2013, 65, 1555-1562.	0.9	4
103	Volcanic history in the Smythii basin based on SELENE radar observation. Scientific Reports, 2019, 9, 14502.	1.6	4
104	Statistical properties of auroral kilometer radiation: based on ERG (ARASE) satellite data. SolneÄno-zemnaâ Fizika, 2021, 7, 11-16.	0.2	4
105	Direct Antenna Impedance Measurement for Quantitative AC Electric Field Measurement by Arase. Journal of Geophysical Research: Space Physics, 2021, 126, e2021JA029111.	0.8	4
106	Study of an equatorward detachment of auroral arc from the oval using groundâ€space observations and the BATSâ€Râ€US – CIMI model. Journal of Geophysical Research: Space Physics, 2021, 126, e2020JA029080.	0.8	4
107	Statistical Study of Approaching Strong Diffusion of Lowâ€Energy Electrons by Chorus and ECH Waves Based on <i>In Situ</i> Observations. Journal of Geophysical Research: Space Physics, 2022, 127, .	0.8	4
108	Asymmetric Distributions of Auroral Kilometric Radiation in Earth's Northern and Southern Hemispheres Observed by the Arase Satellite. Geophysical Research Letters, 2022, 49, .	1.5	4

#	Article	IF	CITATIONS
109	In situ observation atL= 2.3–5 by the Akebono satellite of the plasmaspheric depletion during the September 1998 magnetic storm. Journal of Geophysical Research, 2006, 111, .	3.3	3
110	Statistical studies of fast and slow Z-mode plasma waves in and beyond the equatorial plasmasphere based on long-term Akebono observations. Earth, Planets and Space, 2006, 58, 343-346.	0.9	3
111	Generation mechanism of Z-mode waves in the equatorial plasmasphere. Earth, Planets and Space, 2007, 59, 1027-1034.	0.9	3
112	Comparison of the IRI 2001 model with electron density profiles observed from topside sounder on-board the Ohzora (EXOS-C) and the Akebono (EXOS-D) satellites. Advances in Space Research, 2007, 39, 750-754.	1.2	3
113	GPR observation of the Moon from orbit: Kaguya Lunar Radar Sounder. , 2014, , .		3
114	Seasonal variation of north–south asymmetry in the intensity of Saturn Kilometric Radiation from 2004 to 2017. Planetary and Space Science, 2019, 178, 104711.	0.9	3
115	Detection of UHR Frequencies by a Convolutional Neural Network From Arase/PWE Data. Journal of Geophysical Research: Space Physics, 2020, 125, e2020JA028075.	0.8	3
116	Multievent Study of Characteristics and Propagation of Naturally Occurring ELF/VLF Waves Using High‣atitude Ground Observations and Conjunctions With the Arase Satellite. Journal of Geophysical Research: Space Physics, 2021, 126, e2020JA028682.	0.8	3
117	Localization of Sources of Two Types of Continuum Radiation. JETP Letters, 2021, 114, 23-28.	0.4	3
118	Fieldâ€Aligned Electron Density Distribution of the Inner Magnetosphere Inferred From Coordinated Observations of Arase and Van Allen Probes. Journal of Geophysical Research: Space Physics, 2021, 126, e2020JA029073.	0.8	3
119	First Simultaneous Observation of a Night Time Mediumâ€Scale Traveling Ionospheric Disturbance From the Ground and a Magnetospheric Satellite. Journal of Geophysical Research: Space Physics, 2021, 126, e2020JA029086.	0.8	3
120	Propagation Mechanism of Medium Wave Broadcasting Waves Observed by the Arase Satellite: Hectometric Line Spectra. Journal of Geophysical Research: Space Physics, 2021, 126, e2021JA029813.	0.8	3
121	Simultaneous Observations of EMICâ€Induced Drifting Electron Holes (EDEHs) in the Earth's Radiation Belt by the Arase Satellite, Van Allen Probes, and THEMIS. Geophysical Research Letters, 2022, 49, .	1.5	3
122	Constraint on subsurface structures beneath Reiner Gamma on the Moon using the Kaguya Lunar Radar Sounder. Icarus, 2015, 254, 144-149.	1.1	2
123	Radar Sounding of Subsurface Structure in Eastern Coprates and Capri Chasmata, Mars. Geophysical Research Letters, 2020, 47, e2020GL088556.	1.5	2
124	Overâ€Darkening of Pulsating Aurora. Journal of Geophysical Research: Space Physics, 2021, 126, e2020JA028838.	0.8	2
125	Arase Observation of Simultaneous Electron Scatterings by Upperâ€Band and Lowerâ€Band Chorus Emissions. Geophysical Research Letters, 2021, 48, e2021GL093708.	1.5	2
126	Magnetic Field and Energetic Particle Flux Oscillations and Highâ€Frequency Waves Deep in the Inner Magnetosphere During Substorm Dipolarization: ERG Observations. Journal of Geophysical Research: Space Physics, 2021, 126, e2020JA029095.	0.8	2

#	Article	IF	CITATIONS
127	Geospace Exploration Mission: ERG Project. Transactions of the Japan Society for Aeronautical and Space Sciences Aerospace Technology Japan, 2010, 8, Tm_1-Tm_6.	0.1	2
128	The Lunar Radar Sounder (LRS) Onboard the Kaguya (SELENE) Spacecraft. , 2010, , 145-192.		2
129	Current status and planning of the Plasma Wave Experiment (PWE) onboard the ERG satellite. , 2016, , .		1
130	Simultaneous ground―and satelliteâ€based observation of MF/HF auroral radio emissions. Journal of Geophysical Research: Space Physics, 2016, 121, 4530-4541.	0.8	1
131	Statistical properties of auroral kilometer radiation: based on ERG (ARASE) satellite data. SolneÄno-zemnaâ Fizika, 2021, 7, 13-20.	0.1	1
132	Global Maps of Solar Wind Electron Modification by Electrostatic Waves Above the Lunar Day Side: Kaguya Observations. Geophysical Research Letters, 2021, 48, e2021GL095260.	1.5	1
133	Offâ€Equatorial Pi2 Pulsations Inside and Outside the Plasmapause Observed by the Arase Satellite. Journal of Geophysical Research: Space Physics, 2022, 127, .	0.8	1
134	Vertical plasma extent above the lunar surface derived from interference pattern of auroral kilometric radiation. , 2011, , .		0
135	Observation of plasma waves around the wake of an ionospheric sounding rocket. , 2014, , .		0
136	Study of medium-scale traveling ionospheric disturbances (MSTID) with sounding rockets and ground observations. , 2014, , .		0
137	Temporal and Spatial Variations of Mid-Latitude Ionospheric Trough During a Geomagnetic Storm Based on Global CNSS-TEC and Arase Satellite Observations. , 2018, , .		0
138	Numerical Study of High Frequency Modulation of Electron Precipitation by a Whistler Chorus Element Observed by Arase Satellite. , 2018, , .		0
139	A Sensor Package for Space Weather Global Monitoring Based on Micro Satellite Constellation. Transactions of the Japan Society for Aeronautical and Space Sciences Aerospace Technology Japan, 2018, 16, 687-690.	0.1	0
140	An event study on broadband electric field noises and electron distributions in the lunar wake boundary. Earth, Planets and Space, 2022, 74, .	0.9	0
141	Search for shallow subsurface structures in Chryse and Acidalia Planitiae on Mars. Icarus, 2022, 380, 114991.	1.1	0
142	DEVELOPMENT OF STIFF AND EXTENDIBLE ELECTROMAGNETIC SENSORS FOR SPACE MISSIONS. , 0, , 447-459.		0